

# Auto-regulation of the circadian slave oscillator component *AtGRP7* and regulation of its targets is impaired by a single RNA recognition motif point mutation

Jan C. Schöning<sup>1</sup>, Corinna Streitner<sup>1</sup>, Damian R. Page<sup>2,†</sup>, Sven Hennig<sup>3</sup>, Kenko Uchida<sup>2</sup>, Eva Wolf<sup>3</sup>, Masaki Furuya<sup>2</sup> and Dorothee Staiger<sup>1,\*</sup>

<sup>1</sup>Department of Molecular Cell Physiology, University of Bielefeld, D-33615 Bielefeld, Germany,

<sup>2</sup>Hitachi Advanced Research Laboratory, Hatoyama, Saitama 350-0395, Japan, and

<sup>3</sup>Max-Planck-Institute for Molecular Physiology, D-44202 Dortmund, Germany

Received 3 July 2007; accepted 22 August 2007.

\*For correspondence (fax +49 521 106 6410; e-mail dorothee.staiger@uni-bielefeld.de).

†Present address: archimed medical communication AG, CH-4800 Zofingen, Switzerland.

## Summary

The clock-regulated RNA-binding protein *AtGRP7* (*Arabidopsis thaliana* glycine-rich RNA-binding protein) influences circadian oscillations of its transcript by negative feedback at the post-transcriptional level. Here we show that site-specific mutation of one conserved arginine to glutamine within the RNA recognition motif impairs binding of recombinant *AtGRP7* to its pre-mRNA *in vitro*. This correlates with the loss of the negative auto-regulation *in vivo*: in transgenic plants constitutively overexpressing *AtGRP7* (*AtGRP7-ox*), a shift occurs to an alternatively spliced *AtGRP7* transcript that decays rapidly, and thus does not accumulate to high levels. In contrast, constitutive ectopic overexpression of the *AtGRP7-RQ* mutant does not lead to alternative splicing of the endogenous *AtGRP7* transcript and concomitant damping of the oscillations. This highlights the importance of *AtGRP7* binding to its own transcript for the negative auto-regulatory circuit. Moreover, regulation of *AtGRP7* downstream targets also depends on its RNA-binding activity, as *AtGRP8* and other targets identified by transcript profiling of wild-type and *AtGRP7-ox* plants using fluorescent differential display are negatively affected by *AtGRP7* but not by *AtGRP7-RQ*. In mutants impaired in the nonsense-mediated decay (NMD) components UPF1 or UPF3, levels of the alternatively spliced *AtGRP7* and *AtGRP8* transcripts that contain premature termination codons are strongly elevated, implicating UPF1 and UPF3 in the decay of these clock-regulated transcripts.

**Keywords:** *Arabidopsis*, RNA recognition motif, circadian clock, post-transcriptional regulation, UPF1, UPF3.

## Introduction

In higher plants, a plethora of processes occur once every 24 h (Hall and McWatters, 2006). Orchestrated by an endogenous timekeeper, the circadian clock, these physiological and biochemical processes are optimally aligned with the environmental day/night cycle. This endows plants with enhanced fitness and higher performance (Dodd *et al.*, 2005; Green *et al.*, 2002; McClung, 2006).

It is well established that clock proteins create an auto-regulatory feedback loop and generate their 24 h rhythm by interfering with transcription of their genes. The *Arabidopsis* core clock comprises two Myb-type transcription factors CCA1 and LHY, and the pseudo response regulator TOC1,

that cycle in antiphase and reciprocally regulate each other (Alabadi *et al.*, 2001; Schaffer *et al.*, 1998; Wang and Tobin, 1998). Additional feedback circuits interlock into this basic loop to generate robust oscillations (Locke *et al.*, 2005; Mizuno and Nakamichi, 2005; Salome and McClung, 2005).

Apart from regulating their own expression, clock proteins transduce rhythmicity to produce overt rhythms. They may accomplish this by direct control of downstream genes or via cascades of oscillating gene products (Brown and Schibler, 1999; Staiger *et al.*, 2006). In particular, post-transcriptional control mechanisms have been implicated in shaping rhythmic transcript profiles (Edery, 1999; So and

Rosbash, 1997), but only a few RNA-binding proteins have been shown to be under clock control. The *Drosophila* LARK protein functions in clock output, leading to rhythms in adult eclosion (McNeil *et al.*, 1998), but has an additional non-circadian role in the organization of the actin cytoskeleton during oogenesis (McNeil *et al.*, 2004). Mouse LARK has been implicated in regulation of the clock protein mPERIOD1 (Kojima *et al.*, 2007). It binds to the 3' UTR of the *mPER1* mRNA *in vitro*, and causes elevated mPER1 protein levels, presumably by translational regulation. In *Chlamydomonas reinhardtii*, CHLAMY1 is a heterodimeric RNA-binding protein that binds to UG repeats in the 3' UTRs of several mRNAs *in vitro* and thus mediates translational control, and has been implicated in the control of the phase and period of the clock (Iliev *et al.*, 2006; Zhao *et al.*, 2004).

In Arabidopsis, AtGRP7 operates within an output pathway from the CCA1-LHY-TOC1 clock (Rudolf *et al.*, 2004). Both the transcript and the protein, also designated CCR2 (cold- and circadian-regulated), oscillate with a peak in the subjective evening (Carpenter *et al.*, 1994; Heintzen *et al.*, 1994, 1997). In transgenic plants ectopically overexpressing AtGRP7 under the control of the CaMV 35S promoter, oscillation of endogenous AtGRP7 is strongly depressed, indicating that negative feedback contributes to AtGRP7 rhythmicity (Heintzen *et al.*, 1997). This auto-regulation occurs at the post-transcriptional level, as the use of a cryptic intronic 5' splice site in AtGRP7-ox plants generates a short-lived splice variant (*as\_AtGRP7*) with a premature termination codon (PTC), at the expense of the mRNA (Staiger *et al.*, 2003a).

AtGRP7 has an N-terminal RNA-binding domain of the RNA recognition motif (RRM) type (Figure 1a). This 80-amino-acid domain is composed of a four-stranded anti-parallel  $\beta$ -sheet and two  $\alpha$ -helices, arranged in the order  $\beta 1 \beta 2 \beta 3 \alpha 2 \beta 4$ . The  $\beta 3$  and  $\beta 1$  strands harbour the highly conserved RNP1 (ribonucleoprotein consensus sequence) octapeptide and RNP2 hexapeptide, respectively, which comprise hydrophobic and aromatic residues that make contact with the RNA substrate (Maris *et al.*, 2005). Because recombinant AtGRP7 interacts with its own transcript, alternative splicing and downregulation of the AtGRP7 transcript in response to an elevated protein level may be initiated by AtGRP7 binding to its pre-mRNA (Staiger *et al.*, 2003a).

It is currently not understood whether the AtGRP7 RNA-binding activity does indeed have a functional role in the feedback loop. Our detailed analysis of a protein variant with a mutated RRM shows that a single point mutation that reduces binding affinity *in vitro* is sufficient to disrupt the auto-regulatory circuit *in vivo*, and also interferes with the regulation of downstream targets. Furthermore, we show that the PTC-containing short-lived *as\_AtGRP7* and *as\_AtGRP8* transcripts, which are generated in response to an increasing AtGRP7 protein level, are stabilized in

mutants with reduced *UPF1* or *UPF3* levels, suggesting that components of the NMD pathway are involved in their degradation.

## Results

### *Site-specific mutation of the AtGRP7 RNA recognition motif impairs binding activity*

Binding of AtGRP7 to its pre-mRNA *in vitro* suggests that this interaction, presumably in concert with other factors, causes alternative splicing and concomitant downregulation of endogenous AtGRP7 upon AtGRP7 overexpression. In this scenario, amino acid exchanges interfering with AtGRP7 binding should affect the negative auto-regulation. We chose to replace arginine (R) 49, the first amino acid in the RNP1 consensus sequence, by glutamine (Q) (Figure 1a). Based on alignment of AtGRP7 upon the prototype RRM of human U1A and hnRNP A1, R49 is predicted to lie at the beginning of the  $\beta 3$  strand that forms the RNA-binding platform, and the RQ exchange is expected to impair electrostatic interactions with the RNA (Ding *et al.*, 1999; Jessen *et al.*, 1991; Nagai *et al.*, 1990).

The AtGRP7 target sites within its intron and 3' UTR have been narrowed down by deletion analysis (Staiger *et al.*, 2003a). Oligoribonucleotides (ORN) overlapping these regions (Figure 1b) were synthesized as substrates for RNA band shift assays. Indeed, the ORN derived from the 3' UTR supported binding of GST-AtGRP7 (Figure 1c). In competition assays, 250 pmol of unlabelled 7-UTR\_WT almost completely abrogated AtGRP7 binding, whereas 500 pmol of 7-UTR\_G<sub>4</sub>mut, the corresponding sequence with four guanines exchanged for adenines, influenced binding weakly (Figure S1a). The GST-AtGRP7-RQ mutant protein formed only little shifted complex (Figure 1c). The residual binding activity was competed by the homologous ORN but not by 7-UTR\_G<sub>4</sub>mut, indicating that it retains some sequence preference (Figure S1b). The  $K_d$  for GST-AtGRP7-RQ was about seven times higher than for the WT fusion protein (Figure 1d). This reduced stability of the complex may contribute to the apparent smearing, suggesting partial dissociation during the gel run.

Similarly, the ORN derived from the second half of the intron was sufficient to bind to GST-AtGRP7 (Figure 1e). Increasing amounts of unlabelled 7-intron\_WT reduced complex formation, whereas equal molar excess of the ORN with six guanines exchanged for adenines did not noticeably interfere with complex formation (Figure S2a). Binding of GST-AtGRP7-RQ was strongly reduced (Figure 1e), but was still competed by an excess of unlabelled 7-intron\_WT but not 7-intron\_G<sub>6</sub>mut (Figure S2b). The  $K_d$  value for the interaction of GST-AtGRP7-RQ with the intron was increased about sixfold relative to the  $K_d$  for the WT protein (Figure 1f).

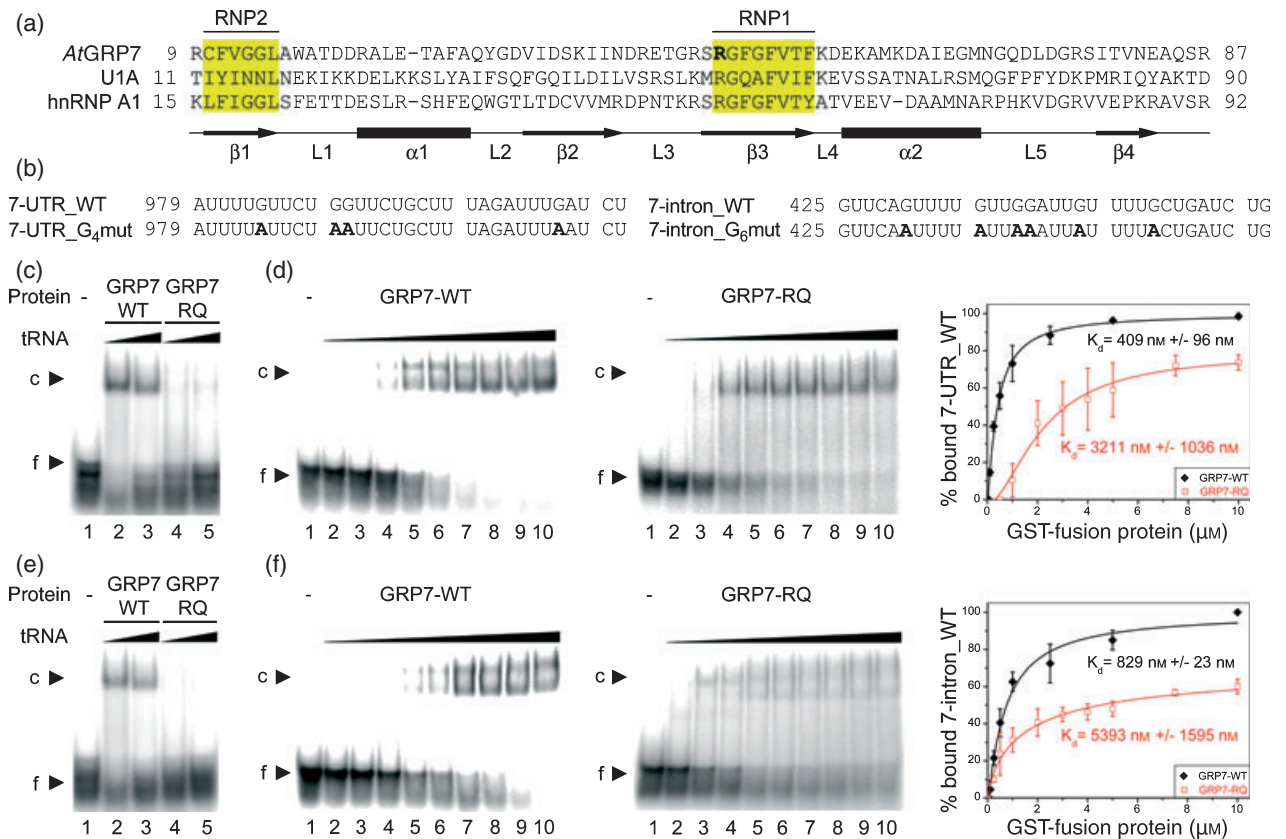


**Figure 1.** Influence of the RNP1 RQ mutation on AtGRP7 binding activity.

(a) AtGRP7 RRM aligned on the N-terminal RRM of U1A and hnRNP A1 (Maris *et al.*, 2005). The conserved RNP1 and RNP2 and predicted secondary structure elements are indicated. The R49 mutated to Q is highlighted in bold. L, loop.

(b) Sequence of the ORN 7-UTR\_WT containing the AtGRP7 binding site within the 3' UTR, mutated 7-UTR\_G4mut with four guanine residues exchanged for adenine (in bold), 7-intron\_WT, and mutated ORN 7-intron\_G6mut with six guanine residues exchanged for adenine (in bold). Numbering is relative to the transcription start site (Staiger and Apel, 1999).

(c) Labelled 7-UTR\_WT was incubated with GST-AtGRP7 (lanes 2 and 3) or GST-AtGRP7-RQ (lanes 4 and 5) and 1 μg (lanes 2 and 4) or 10 μg (lanes 3 and 5) of tRNA. Lane 1, free ORN (f). c, RNA-protein complex.

(d) To compare binding affinities of WT and mutant protein, 50 fmol of labelled 7-UTR\_WT were incubated with 0.01, 0.05, 0.1, 0.25, 0.5, 1, 2.5, 5 or 10 μM of GST-AtGRP7 (left, lanes 2–10, respectively) or 0.5, 1, 2, 3, 4, 5, 7.5, 10 or 20 μM of GST-AtGRP7-RQ (middle, lanes 2–10, respectively), in the presence of 1 μg tRNA. Bound and free RNA levels were quantified (right), and  $K_d$  values were calculated based on three independent experiments as described in Experimental procedures.

(e) Labelled 7-intron\_WT was incubated with GST-AtGRP7 (lanes 2 and 3) or GST-AtGRP7-RQ (lanes 4 and 5) and 1 μg (lanes 2 and 4) or 10 μg (lanes 3 and 5) of tRNA. Lane 1, free ORN.

(f) To compare binding affinities of WT and mutant protein, 50 fmol of labelled 7-intron\_WT were incubated with 0.01, 0.05, 0.1, 0.25, 0.5, 1, 2.5, 5 or 10 μM of GST-AtGRP7 (left, lanes 2–10, respectively) or 0.25, 0.5, 1, 2, 3, 4, 5, 7.5 or 10 μM of GST-AtGRP7-RQ (middle, lanes 2–10, respectively), in the presence of 1 μg tRNA.  $K_d$  values were determined as in (d).

To confirm that the RQ exchange does not interfere with protein folding, circular dichroism spectra were recorded (Figure S3). The band at 208 nm and the shallow minimum around 222 nm indicate the presence of separate  $\alpha$ -helical and  $\beta$ -sheet regions consistent with the typical RRM structure. The spectra of AtGRP7 WT and AtGRP7-RQ mutant proteins were almost undistinguishable, strongly suggesting that the reduced affinity of AtGRP7-RQ for RNA is not due to unfavourable secondary structure of the  $\beta$  strand harbouring mutated RNP1. Thus, the R49 mutation severely interferes with binding of recombinant AtGRP7 to both the 3' UTR and intron.

#### Overexpression of the AtGRP7-RQ variant does not cause alternative splicing of endogenous AtGRP7

To test the impact of the RQ mutation on AtGRP7 activity *in vivo*, the AtGRP7-RQ protein was constitutively overexpressed under the control of the CaMV promoter. Transgenic plants were identified with a total AtGRP7 transcript level similar to that in AtGRP7-ox plants of both the Col and C24 ecotypes (Figure 2a, top). An immunoblot analysis confirmed that the mutated protein was stably expressed, as total AtGRP7 protein was elevated to a level similar to that in AtGRP7-ox plants (Figure 2b). However, in contrast to

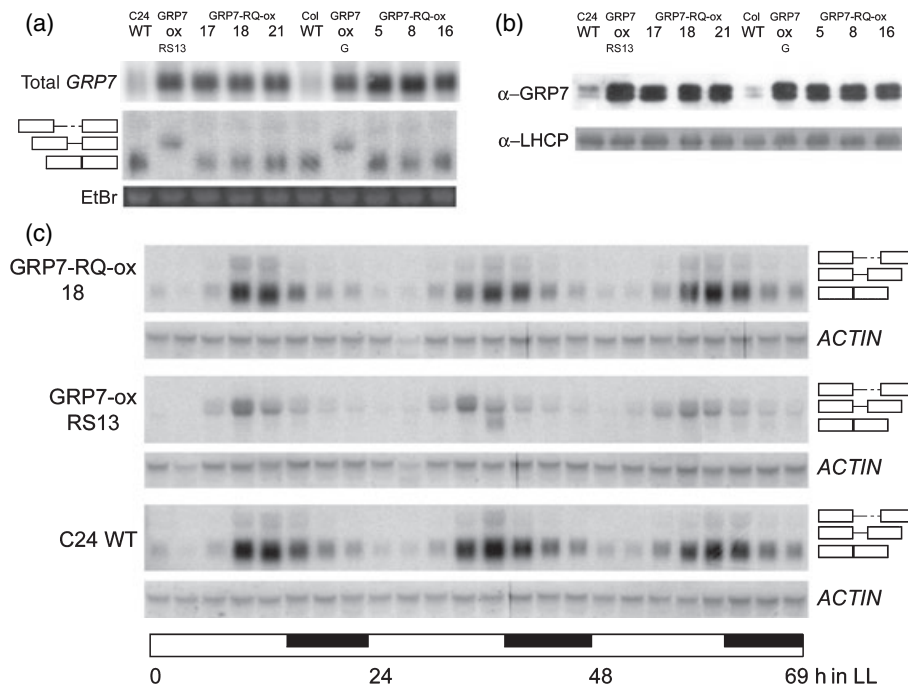


**Figure 2.** The AtGRP7-RQ mutant protein does not feed back on endogenous *AtGRP7*.

(a) *AtGRP7-RQ-ox* plants in the C24 and Col background as well as the corresponding *AtGRP7-ox* and WT plants were harvested at zt12. The RNA gel blot was hybridized with *AtGRP7* cDNA to determine the total transcript level (top) and with a gene-specific probe to detect the level of endogenous *AtGRP7* transcript (middle). The positions of the pre-mRNA, as *AtGRP7* retaining the first half of the intron, and the mRNA are indicated. Boxes represent exons, and the solid and broken lines represent the first and second halves of the intron, respectively. The ethidium bromide-stained gel shows equal loading (bottom).

(b) The immunoblot of the same samples as in (a) was incubated with an antibody against *AtGRP7* (top). The double band may reflect proteolytic degradation or post-translational modification. Subsequently, the blot was probed with an antibody against light harvesting chlorophyll binding protein (LHCP) as a loading control (bottom).

(c) C24 WT, *AtGRP7-ox* (line RS13) and *AtGRP7-RQ-ox* plants (line 18) were harvested at 3 h intervals after transfer to LL. The endogenous *AtGRP7* transcript was detected using a gene-specific probe (top). Hybridization with *ACTIN* served as constitutive control (bottom).

*AtGRP7-ox* plants, the endogenous *AtGRP7* transcript remained at the same level as in WT (Figure 2a, middle). An extended time course assay in plants shifted to constant light (LL) after entrainment under light/dark cycles (LD) showed that, in *AtGRP7-RQ-ox* plants, oscillations of the endogenous *AtGRP7* mRNA were more or less indistinguishable from that in WT (Figure 2c). Thus, *AtGRP7-RQ* does not cause a shift in the splice site with concomitant reduction in transcript abundance, as observed in *AtGRP7-ox* control plants. We infer from this that the weakened interaction of *AtGRP7-RQ* with its own RNA prevents efficient negative auto-regulation of the *AtGRP7* pre-mRNA.

#### *AtGRP7* targets comprise circadianly and non-circadianly regulated transcripts

Targets of *AtGRP7* regulation are expected to be affected by constitutive *AtGRP7* overexpression. Therefore, transcript profiles from WT and *AtGRP7-ox* plants were compared by fluorescent differential display (FDD). To exclude non-specific effects as much as possible, we used two growth conditions, namely soil and agar plates. Aerial parts of plants of

identical size each were harvested at the subjective circadian maximum of *AtGRP7*, in the evening, and at the subjective minimum, in the morning, on the first and second day in LL, respectively. Total RNA was reverse-transcribed using fluorescent-labelled 3'-anchored oligo(dT) primers terminating in A or C, and the cDNAs were subjected to amplification using 140 arbitrary 10-mer primers, each combined with the respective anchor primer. Among approximately 50 000 displayed bands showing a difference under both conditions, 28 showed differences upon re-testing. Analysis by PCR revealed that several transcripts with higher abundance in *AtGRP7-ox* plants were derived from the transgene. Conversely, several bands with lower abundance in *AtGRP7-ox* plants corresponded to *AtGRP8*, which encodes a related RNA-binding protein that is under negative control by *AtGRP7* (Heintzen *et al.*, 1997). Six of the remaining eight fragments showed only a minor difference (not shown).

Figure S4 shows the FDD pattern for a band identified in circadian minimum RNA using arbitrary primer A3 (AGT-CAGCCAC). The transcript is strongly expressed in C24 and Col harvested at zt0 (Zeitgeber time), zt6 and zt12, but is reduced in *AtGRP7-ox* plants of the C24 ecotype (line RS13)

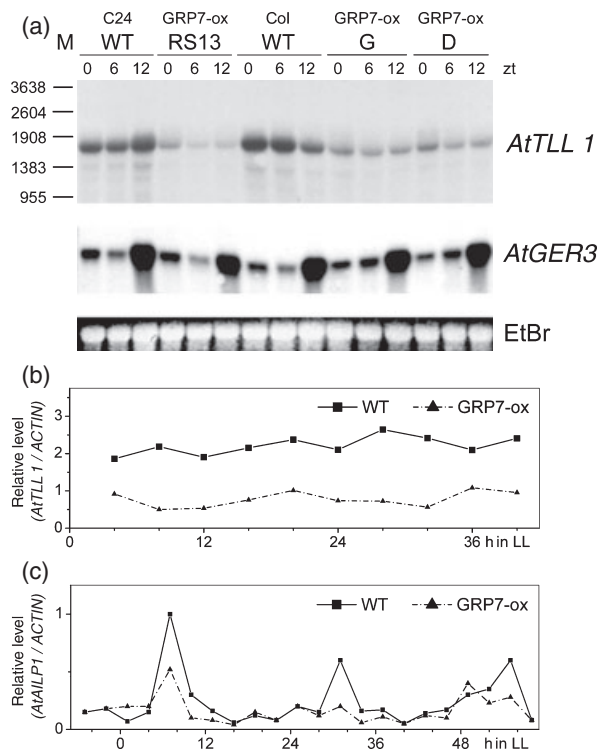


**Figure 3.** Differential expression of *AtTLL1* and *AtAILP1* in *AtGRP7*-ox plants. (a) *AtGRP7*-ox plants in the C24 (line RS13) and Col backgrounds (lines D and G) and WT plants raised under LD conditions were harvested at zt0, zt6 and zt12. The RNA gel blot was hybridized with *AtTLL1* (top) and *AtGER3* (middle; Staiger *et al.*, 1999). The positions of RNA size markers are indicated. The ethidium bromide-stained gel shows equal loading (bottom). (b) *AtGRP7*-ox and WT plants were raised under LD conditions and subsequently shifted to LL conditions. Plants were harvested at 4 h intervals starting 4 h after lights on (LL4). Hybridization signals for *AtTLL1* were normalized to *ACTIN* levels. (c) *AtGRP7*-ox and WT plants were raised under LD conditions and subsequently shifted to LL conditions. Plants were harvested at 3 h intervals starting 5 h before lights on (zt19). Hybridization signals for *AtAILP1* were normalized to *ACTIN* levels.

and Col ecotype (lines D and G), indicating that an elevated *AtGRP7* protein level leads to reduced steady-state mRNA abundance (Figure 3a). The *AtGER3* transcript, which encodes a circadian-regulated germin-like protein with an evening peak (Staiger *et al.*, 1999) and which was used as a control, is not affected (Figure 3b).

Sequence analysis revealed that the cDNA fragment is derived from At1g45201, covering about 150 amino acids of the last two exons as well as the 3' UTR. The deduced ORF encodes a 54 kDa protein with a putative signal peptide for the endomembrane system and three transmembrane domains. Based on its homology to lipase class 3 proteins, it is predicted to have triacylglycerol lipase activity and was designated *AtTLL1* (*Arabidopsis thaliana* triacylglycerol lipase-like). To test its temporal expression pattern, an RNA time course assay was performed using WT and *AtGRP7*-ox plants shifted to LL after LD entrainment. *AtTLL1*

mRNA levels were not constant across the day but did not show obvious circadian oscillations (Figure 3b). The expression in the transgenic plants was consistently reduced compared with WT.

Another transcript identified using primer X5 (CCTTT-CCCTC) was weakly down-regulated in *AtGRP7*-ox plants. Sequencing revealed homology to the last exon and the 3' UTR of At5g19140, which encodes a 25-kDa protein with a predicted chloroplast transit peptide. It harbours a domain with similarity to an Ntn (N-terminal nucleophile aminohydrolase) domain, and is highly homologous to aluminium-induced proteins in *Brassica napus*, *Phaseolus aureus* and *Gossypium hirsutum*. We found that this *AtAILP1* (*Arabidopsis thaliana* aluminium-induced-like protein) transcript undergoes circadian oscillations with a maximum in the middle of the day, and the peak in *AtGRP7*-ox plants is reduced about twofold compared with WT (Figure 3c).

#### The *AtGRP7*-RQ mutation impairs *AtGRP7* target regulation

To determine whether the reduced RNA-binding activity of *AtGRP7*-RQ also interfered with regulation of its downstream targets, we compared the levels of the various *AtGRP8* splice variants with those in WT and *AtGRP7*-ox plants. In *AtGRP7*-RQ-ox plants, the *AtGRP8* mRNA and the pre-mRNA were present at levels similar to that in WT, and only a faint band corresponding to the alternatively spliced *AtGRP8* (as-*AtGRP8*) was detected (Figure 4a). An extended time course assay showed that the oscillation of *AtGRP8* in *AtGRP7*-RQ-ox plants was similar to that in WT, whereas only the as-*AtGRP8* RNA was detected in *AtGRP7*-ox plants, and this oscillated at a reduced level (Figure 4c). This indicates that mutation of R49 almost completely abrogated the ability of *AtGRP7* to influence the choice between the regular and the cryptic 5' splice site in the *AtGRP8* transcript also, followed by rapid decay of the alternative splice form. Moreover, in *AtGRP7*-RQ-ox plants, the *AtGRP8* protein remained at WT levels, whereas it was strongly reduced in *AtGRP7*-ox plants (Figure 4b).

In addition, the *AtTLL1* level, which was strongly reduced in *AtGRP7*-ox line G relative to Col WT, was only weakly affected in *AtGRP7*-RQ-ox line 5 (Figure 5a). Quantitative real-time PCR of several independent transgenic lines further demonstrated that, in *AtGRP7*-ox plants, its level was reduced relative to that in WT, whereas it was only weakly affected in *AtGRP7*-RQ-ox plants (Figure 5b). For *AtAILP1*, quantitative real-time PCR confirmed that its peak abundance was strongly reduced in *AtGRP7*-ox plants but only moderately affected in *AtGRP7*-RQ-ox plants (Figure 5c). Taken together, the reduced RNA-binding activity of *AtGRP7* caused by the single RQ exchange impairs regulation of its downstream targets *AtGRP8*, *AtTLL1* and *AtAILP1*.

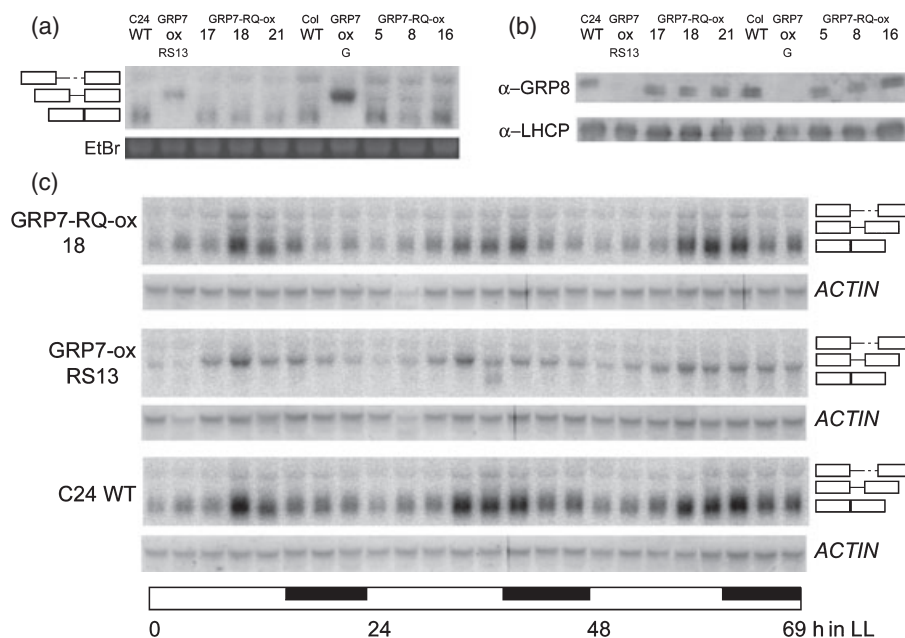


**Figure 4.** The AtGRP7-RQ mutant interferes with regulation of *AtGRP8*.

(a) AtGRP7-RQ-ox plants in the C24 and Col backgrounds as well as the corresponding AtGRP7-ox and WT plants were harvested at zt12. The RNA gel blot was hybridized with the gene-specific *AtGRP8* probe (top). The positions of the pre-mRNA, the alternatively spliced transcript *as-AtGRP8* retaining the first half of the intron, and the mRNA are indicated. Boxes represent exons, and the solid and broken lines represent the first and second halves of the intron, respectively. The ethidium bromide-stained gel shows equal loading (bottom).

(b) The immunoblot of the same samples as in (a) was incubated with an antibody against AtGRP8.

(c) WT C24, AtGRP7-ox (line RS13) and AtGRP7-RQ-ox (line 18) plants entrained under LD conditions were harvested at 3 h intervals after transfer to LL. The *AtGRP8* transcript was detected using a gene-specific probe on the blot previously hybridized with *AtGRP7* (see Figure 2c) (top). Hybridization with *ACTIN* served as constitutive control (bottom).

#### *AtGRP7* binding to *AtGRP8*

To investigate whether *AtGRP7* directly interacts with the *AtGRP8* pre-mRNA, we searched for potential *AtGRP7* binding sites using sequence homology analysis (Clustal W and Dialign) and secondary structure prediction tools (mfold and RNA-shapes; Morgenstern, 2004; Steffen *et al.*, 2006; Thompson *et al.*, 1994; Zuker, 2003). Regions displaying similarity to the *AtGRP7* intron and 3' UTR binding sites were identified in analogous positions within the *AtGRP8* transcript. The corresponding regions, as well as mutant variants with defined base exchanges, were synthesized as ORN (Figure 6a). Strong complex formation was observed between *AtGRP7* and 8-UTR\_WT, whereas the *AtGRP7*-RQ mutant formed almost no retarded complex (Figure 6b). Binding was reduced by unlabelled homologous 8-UTR\_WT but not by an ORN carrying six guanine mutations, indicating specific binding (Figure S5).  $K_d$  measurements revealed a ninefold reduced affinity of *AtGRP7*-RQ (Figure 6c). With 8-intron\_WT, weaker complex formation was observed (Figure 6d), which was more strongly competed by the homologous unlabelled ORN than by the 8-intron\_G<sub>2</sub>U<sub>2</sub>mut with two guanines and two uracils mutated (Figure S6a). Mutation of R49 almost completely eliminated binding to 8-intron\_WT (Figure 6e and Figure S6b). In contrast, no

obvious *AtGRP7* target sites were identified *in silico* for *AtTLL1* and *AtAIP1*, suggesting that they could be regulated indirectly by *AtGRP7*.

#### *Involvement of UPF1 and UPF3 in as-AtGRP7 and as-AtGRP8 decay*

The *as-AtGRP7* transcript that is produced as a result of negative auto-regulation has a short half-life. Because it harbours a PTC within the retained first half of the intron, we investigated whether its degradation may involve NMD. In mammals, UPF3 (UP-FRAMESHIFT PROTEIN) is part of the large exon junction complex (EJC) deposited on mRNAs during splicing 20–24 nt upstream of an exon–exon boundary. In an aberrant transcript, the translating ribosomes encounter a stop codon upstream of an EJC. The UPF1 helicase that is recruited by the translation release factors then interacts with the EJC, targeting the mRNA for degradation. The mechanism of NMD and the *cis*-acting signals involved are not well understood in plants as yet (Kertesz *et al.*, 2006). A T-DNA mutant in the Arabidopsis UPF3 homologue has been found to accumulate alternative splicing products with PTCs (Hori and Watanabe, 2005), and several mRNAs containing PTCs are enriched in T-DNA mutants of the Arabidopsis UPF1 homologue (Arciga-Reyes

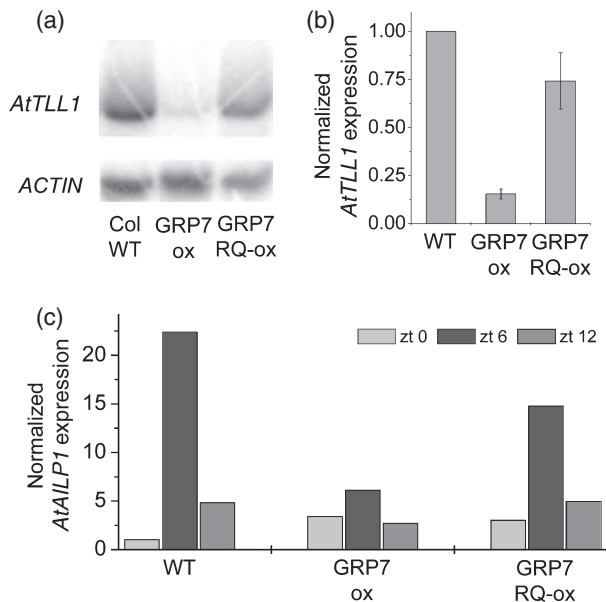


**Figure 5.** The AtGRP7-RQ mutation interferes with AtTLL1 and AtAILP1 regulation.

(a) Blot with RNAs from Col WT, AtGRP7-ox and AtGRP7-RQ-ox plants harvested at zt12 hybridized with AtTLL1 (top) and ACTIN (bottom).

(b) Quantitative real-time PCR was performed on RNA from plants harvested at zt12. The AtTLL1 expression level in the transgenic plants was normalized to that for the WT in each experiment with respect to the PPR or eIF-4A-1 reference genes. Shown are the average values of the AtGRP7-RQ-ox lines 17 and 18 in C24, the AtGRP7-RQ-ox lines 5 and 16 in Col, the corresponding WT lines, and the AtGRP7-ox line RS13 in C24 and line G in Col, analysed in three independent experiments. Error bars represent standard deviations.

(c) Quantitative RT-PCR was performed on RNA from plants harvested at zt0, zt6 and zt12. The AtAILP1 expression level in the transgenic plants was normalized to the level of C24 at zt0 with respect to the eIF-4A-1 reference gene.

*et al.*, 2006). Using RT-PCR followed by hybridization with radiolabelled AtGRP7 cDNA, we found that the level of as-AtGRP7 was elevated weakly in the *upf1-4* mutant and very strongly in *upf1-5*. It was also higher in *upf3-1* and *upf3-2* mutants than in WT (Figure 7). Similarly, as-AtGRP8 steady-state abundance was elevated in both *upf1* and *upf3* mutants but ACTIN was not affected. Both UPF1 and UPF3 thus participate in the decay of the transcripts that are produced when the level of AtGRP7 protein is high.

## Discussion

### An RNP1 R49Q mutation impairs AtGRP7 in vitro binding activity

To demonstrate that binding of AtGRP7 to its pre-mRNA is inherent in the negative feedback loop, we aimed to correlate AtGRP7 *in vitro* binding activity with its activity *in vivo*. Exchange of a conserved arginine in RNP1 increased the  $K_d$  value about fivefold for both the 3' UTR and intron target

sites. The almost identical CD spectra of WT and mutant protein exclude the possibility that the reduced affinity for RNA is due to improper folding.

RNA contacts for the RNP1 arginine were first identified in the crystal structure of the U1A RRM complexed with U1 snRNA (Nagai *et al.*, 1990). Replacement of R52, the AtGRP7 R49 equivalent, by glutamine abolished binding of the U1A RRM to the U1 stem-loop II, implicating the R52 side chain in salt bridges with the phosphate backbone (Jessen *et al.*, 1991). Molecular dynamics simulation of the U1A-U1 stem-loop II complex revealed that R52 is indeed a crucial residue involved in electrostatic and hydrogen-bonding interactions (Tang and Nilsson, 1999). Similarly, surface plasmon resonance studies to monitor the kinetics of U1A association with U1 stem-loop II have attributed an initiating role to R52 in the close-range interactions (Law *et al.*, 2005). Also, in both RRM of hnRNP A1 and the second RRM of *Drosophila* SEX-LETHAL, arginines occupying the analogous position to AtGRP7 R49 make important contacts with the respective targets (Ding *et al.*, 1999; Lee *et al.*, 1997).

Although no structural data are available for plant glycine-rich RNA-binding proteins complexed to RNA, the decrease in binding strength upon site-specific mutation of the AtGRP7 RNP1 arginine suggests that the arginine makes important contacts with its targets in this plant RRM protein also. The observation that the residual binding activity of AtGRP7-RQ has the same sequence preference as the WT protein suggests that R49 has a function during complex formation but not for target selection.

### Functional relevance of AtGRP7 R49 in vivo

We show here that mutation of the conserved R49 disrupts AtGRP7 activity. The *in vivo* effect of a single RNP1 arginine mutant was previously analysed for SANSFILLE (SNF), the *Drosophila* homologue of U1A and U2B'' that harbours two RRM and binds to both U1 snRNA and U2 snRNA (Stitzinger *et al.*, 1999). The lethal *snf* phenotype is rescued by expressing an SNF-R49Q mutant protein. Although the RQ mutation of the N-terminal RRM is predicted to eliminate RNA binding, SNF-R49Q still associates with both U1 and U2 snRNAs. Thus, in the otherwise intact SNF protein, the C-terminal RRM can obviously provide other contacts for snRNP assembly, and an essential role for the arginine *in vivo* was not identified (Stitzinger *et al.*, 1999).

In contrast, the reduced binding activity of AtGRP7 protein upon R49Q mutation directly manifests itself *in vivo*. We conclude that the arginine makes important contacts with the RNA targets such that the R49Q mutation has a strong effect on the negative auto-regulation and on the regulation of downstream targets *in vivo*. Single-RRM proteins such as AtGRP7 may thus provide some advantage for simultaneous mutational analysis of binding requirements and *in vivo* function.

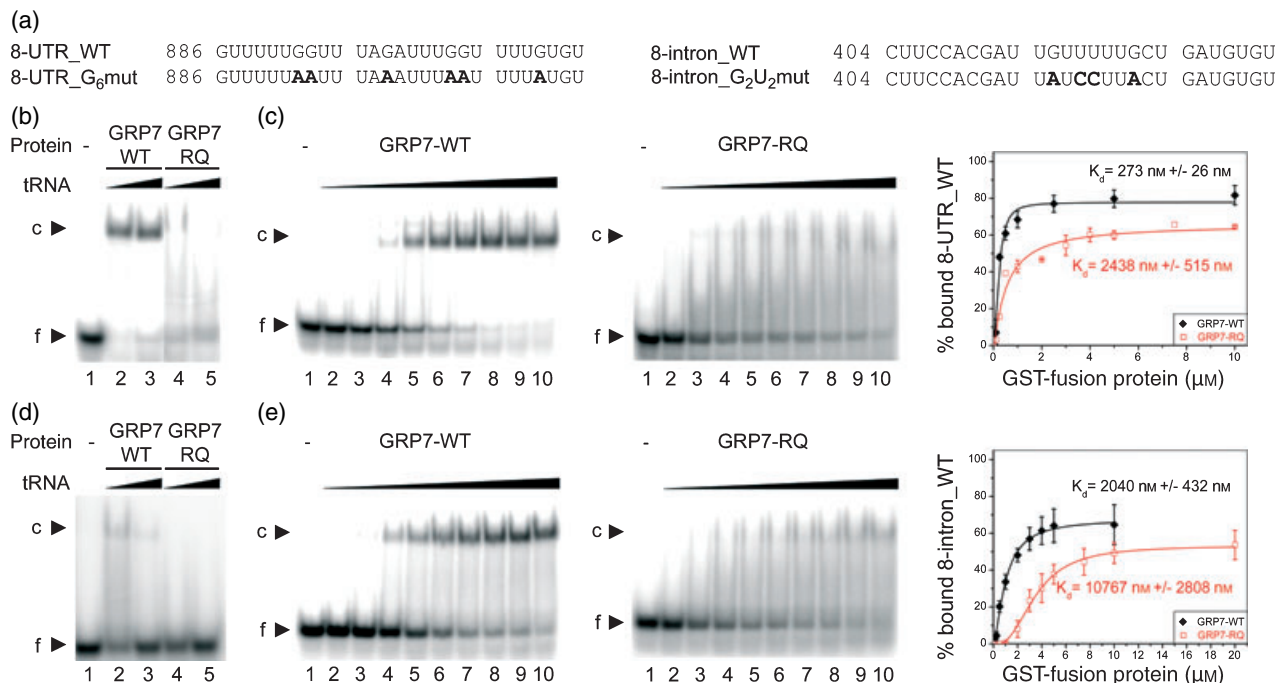


**Figure 6.** Influence of the RNP1 RQ mutation on AtGRP7 binding to the AtGRP8 intron and 3' UTR.

(a) Sequence of the AtGRP8 3' UTR and intron ORN and the corresponding mutated 8-UTR\_G<sub>6</sub>mut and 8-intron\_G<sub>2</sub>U<sub>2</sub>mut with six guanine residues exchanged for adenine or two guanine and two uracil residues exchanged for adenine or cytosine (in bold), respectively. Numbering is relative to the start site of transcription (Staiger, unpublished data).

(b, d) The labelled 8-UTR\_WT (b) and 8-intron\_WT (d) ORN were incubated with GST-AtGRP7 (lanes 2 and 3) or GST-AtGRP7-RQ (lanes 4 and 5) and 1 μg (lanes 2 and 4) or 10 μg (lanes 3 and 5) of tRNA, respectively. Lane 1, free ORN.

(c) To compare binding affinities of WT and mutant protein, 50 fmol of labelled 8-UTR\_WT ORN were incubated with 0.01, 0.05, 0.1, 0.25, 0.5, 1, 2.5, 5 or 10 μM of GST-AtGRP7 (left, lanes 2–10, respectively) or GST-AtGRP7-RQ (middle, lanes 2–10, respectively). Bound and free RNA levels were quantified, and K<sub>d</sub> values were calculated based on the mean of three independent experiments as described in Experimental procedures.

(e) To compare binding affinities of WT and mutant protein, 50 fmol of labelled 8-intron\_WT ORN were incubated with 0.1, 0.25, 0.5, 1, 2, 3, 4, 5 or 10 μM of GST-AtGRP7 (left, lanes 2–10, respectively) or 1, 2, 3, 4, 5, 7.5, 10 or 20 μM of GST-AtGRP7-RQ (middle, lanes 2–10, respectively). All reactions contain 1 μg tRNA. Bound and free RNA levels were quantified, and K<sub>d</sub> values were calculated based on the mean of three independent experiments as described in Experimental procedures.

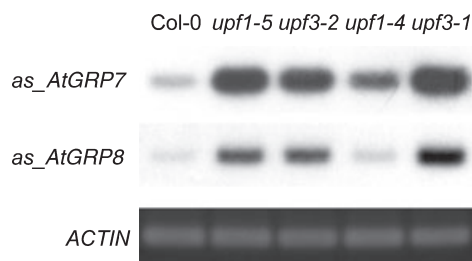


**Figure 7.** Effect of upf1 and upf3 on steady-state abundance of the alternatively spliced AtGRP7 and AtGRP8 transcripts.

RNA from the mutants and Col WT harvested at zt10 was reverse-transcribed. PCR amplification of the as\_AtGRP7 and as\_AtGRP8 transcripts was performed using specific primers (listed in Table S1) and 24 cycles. The gel with the PCR products was blotted and hybridized with AtGRP7 (top) and AtGRP8 (middle) cDNAs. The exponential range was determined by comparing the signal over increasing numbers of cycles. Amplification with ACTIN primers served as a control (bottom).

It should be noted that the R49Q mutation may have additional consequences that are not revealed by these *in vitro* binding assays, for example in protein-protein

interactions. However, participation of the RNP1 arginine in such an interaction has not been described so far (Maris *et al.*, 2005).

#### Impact of the AtGRP7 RNP1 R49Q mutation on target gene regulation

The R49Q mutation also abolishes the influence of AtGRP7 on alternative splicing of AtGRP8 and concomitant down-regulation of the AtGRP8 protein. As recombinant AtGRP7 specifically binds to both the AtGRP8 intron and 3' UTR in a manner dependent on R49, it is conceivable that AtGRP7 directly binds to the AtGRP8 transcript to depress its abundance at the post-transcriptional level.

Transcript profiling of AtGRP7-ox and WT plants uncovered an additional transcript, AtTLL1, that is negatively regulated by AtGRP7. The deduced amino acid sequence shows homology to class 3 lipases. It harbours the active site of triacylglycerol (TAG) lipases comprising a triad Ser-Asp/Glu-His and the conserved pentapeptide GX<sub>S</sub>XG. AtTLL1 shows about 39% sequence identity to an acid

lipase from castor bean that is associated with the oil body membrane (Eastmond, 2004), and is a member of a small gene family of unknown function. Lipase-like proteins have also been implicated in pathogen defence responses (Falk *et al.*, 1999; Jakab *et al.*, 2003). In contrast to *AtGRP7* and *AtGRP8*, no binding of *AtGRP7* to the 3' UTR of *AtTLL1* was demonstrated, and no obvious intronic binding sites were identified *in silico* (not shown). Thus, *AtGRP7* may exert its control on *AtTLL1* indirectly by influencing processing of an mRNA coding for a *trans*-acting regulator.

A second newly described *AtGRP7* target transcript, *AtAILP1*, which shows homology to aluminium-induced transcripts in other plants, undergoes circadian oscillations, and the peak abundance is reduced in *AtGRP7-ox* but not *AtGRP7-RQ ox* plants. This transcript is induced by several external stimuli (Zimmermann *et al.*, 2004). Taken together, these observations implicate *AtGRP7* in the regulation of both rhythmic and non-rhythmic transcripts.

In mammals, the circadian-regulated DBP, TEF and HLF transcription factors are prime examples of output mediators that are activated by the core oscillator at the transcriptional level but do not feedback onto clock gene expression (Gachon *et al.*, 2004). Transcript profiling of triple knockout mice has identified downstream targets with rhythmic as well as constant expression patterns (Gachon *et al.*, 2006). The identification of an *AtGRP7* target transcript showing no obvious circadian oscillation may also be related to an additional function. For example, *AtGRP7* has been implicated in ABA and stress signalling, as an *atgrp7* mutant accumulated higher levels of the ABA- and stress-inducible *RD29A* transcript (Cao *et al.*, 2006). We found a reduction of *RD29A* in *AtGRP7-ox* but not *AtGRP7-RQ-ox* plants (data not shown). Notably, *RD29A* is also regulated by the circadian clock (Dodd *et al.*, 2006; Edwards *et al.*, 2006).

#### *UPF1 and UPF3 influence as<sub>AtGRP7</sub> and as<sub>AtGRP8</sub> levels*

Negative auto-regulation of *AtGRP7* involves the generation of *as<sub>AtGRP7</sub>* with a PTC in the retained part of the intron. To begin to identify components responsible for *as<sub>AtGRP7</sub>* degradation, we analysed its level in *upf1* and *upf3* mutants. UPF1 and UPF3 are critical components for NMD in yeast, *Drosophila*, humans and worms (Chang *et al.*, 2007). Recently, the Arabidopsis orthologues have been implicated in the degradation of PTC-containing transcripts (Arciga-Reyes *et al.*, 2006; Hori and Watanabe, 2005). We found that *as<sub>AtGRP7</sub>* is elevated in the *upf1-4* and *upf1-5* mutants, indicating that UPF1 is required for its degradation. Notably, the increase was much higher in *upf1-5* than in *upf1-4*, consistent with a more reduced level of UPF1 in *upf1-5* (Arciga-Reyes *et al.*, 2006). UPF3

was identified as another component required for degradation of *as<sub>AtGRP7</sub>*, as the level of *as<sub>AtGRP7</sub>* was higher in the *upf3-1* and *upf3-2* mutants compared with WT. Furthermore, *as<sub>AtGRP8</sub>* is also elevated in each mutant. Recently, alternative branches of the NMD pathway have been shown to occur independently of a particular UPF protein (Chang *et al.*, 2007). The finding that mutants with reduced levels of either UPF1 or UPF3 have higher levels of *as<sub>AtGRP7</sub>* and *as<sub>AtGRP8</sub>* suggest that they indeed may be targeted to the NMD pathway. As NMD depends on translation, NMD targets are enriched by translation inhibition. Consistent with this, we found that cycloheximide stabilizes *as<sub>AtGRP7</sub>* (Staiger *et al.*, 2003a) and *as<sub>AtGRP8</sub>* (unpublished observation) in *AtGRP7-ox* plants, and thus mimics NMD mutants. Furthermore, upon cycloheximide treatment, *as<sub>AtGRP7</sub>* and *as<sub>AtGRP8</sub>* did not accumulate in the *upf* mutants beyond the level in WT (not shown). Interestingly, developmental phenotypes were observed in *upf1* and *upf3* mutants, and thus NMD components apparently have a widespread role in co-ordinated gene expression during regular development (Arciga-Reyes *et al.*, 2006; Hori and Watanabe, 2005). In this context, our data suggest a link between post-transcriptional regulation in the circadian clock system and UPF-dependent RNA decay.

In conclusion, our data correlate the importance of the conserved RNP1 arginine for *AtGRP7* binding to *AtGRP7* and *AtGRP8* pre-mRNAs with a crucial role of *AtGRP7* in the negative auto-regulatory circuit and the regulation of several downstream targets.

Interestingly, *AtGRP7* R49 is a target of a novel virulence strategy deployed by *Pseudomonas syringae*. The type III effector HopU1 is an ADP-ribosyltransferase that modifies *AtGRP7* in a manner dependent on R47 and R49 (Fu *et al.*, 2007). This suggests that HopU1 may interfere with post-transcriptional processes in the host cell by inhibiting the ability of *AtGRP7* to bind RNA and thus quell plant immune responses. Our findings suggest a way to further investigate how this RNA-binding protein controls target transcripts, both as part of a signalling cascade downstream of the circadian oscillator and in processes that are not dependent on clock regulation.

## Experimental procedures

### *Oligonucleotide-directed mutagenesis*

The conserved arginine residue in RNP1 was exchanged for glutamine by PCR with Pfu turbo polymerase (Stratagene, <http://www.stratagene.com/>) using the overlapping primers *RQ<sub>for</sub>* (5'-ACTGGAAGATCCCAAGATTTCGATTCGTCACCTT-3') and *RQ<sub>rev</sub>* (5'-AATCGAATCCTTGGGATCTCCAGTCTCACGATC-3'). Silent mutations were introduced into neighbouring amino acids, creating a diagnostic *StyI* restriction site (underlined). The mutation was verified by sequencing.

### Recombinant glutathione S-transferase-AtGRP7

Intact RNP1 in the plasmid pGST-AtGRP7 was replaced by RNP1-RQ using flanking restriction sites. WT and mutant fusion proteins were expressed in *Escherichia coli* BL21 cells and purified as described previously (Staiger *et al.*, 2003a).

### RNA electrophoretic mobility shift assays

Synthetic ORN (Figures 1b and 7a) were obtained from Biomers (<http://www.biomers.net>), and end-labelled using T4 polynucleotide kinase and  $\gamma$ [<sup>32</sup>P]ATP. Binding assays containing 50 fmol of labelled ORN and 0.5  $\mu$ g of recombinant GST-AtGRP7 were performed as described previously (Staiger *et al.*, 2003a). The dried polyacrylamide gels were analysed using a Typhoon 8000 phosphorimager and ImageQuant software (Amersham Pharmacia Biotech, <http://www5.amershambiosciences.com/>). For determination of equilibrium dissociation constants ( $K_d$ ), increasing amounts of protein were incubated with 50 fmol of labelled ORN. Three independent experiments were performed and the results are given as means  $\pm$  SEM. The log (complexed/free probe) of the mean curve was plotted against the log (protein concentration). The x intercept corresponds to the log ( $K_d$ ).

### Circular dichroism

GST-AtGRP7 and GST-AtGRP7-RQ in pGEX-6P1 (GE Healthcare; <http://www.gelifesciences.com>) were eluted from a glutathione-Sepharose column using 20 mM glutathione, followed by PreScission™ (GE Healthcare; <http://www.gelifesciences.com>) protease cleavage. The AtGRP7 moieties were further purified on an ÄKTA Explorer system (GE Healthcare; <http://www.gelifesciences.com>) using an HR 10/30 Superdex 75 column (Amersham Biosciences) pre-equilibrated with 20 mM NaH<sub>2</sub>PO<sub>4</sub>, pH 7.7, and 20 mM Na<sub>2</sub>SO<sub>4</sub>. The purified protein was diluted to 10  $\mu$ M. CD spectra were measured using a Jasco J-815 spectropolarimeter (Jasco; <http://www.jasco-europe.com>), and represent the mean molar ellipticity per amino acid residue of protein after buffer correction. Data were collected at 10°C from 190 to 260 nm with 0.2 nm intervals, collecting data for 1 sec at each point. For each measurement, 10 spectra were used for accumulation.

### Transgenic plants

To overexpress the AtGRP7-RQ mutant protein, RNP1 in the expression plasmid harbouring the AtGRP7 coding region under the control of the CaMV promoter with duplicated enhancer and the omega element (Heintzen *et al.*, 1997) was replaced by RNP1-RQ using flanking restriction sites. The expression cassette was subcloned into pBin19 and transformed into Arabidopsis as described previously (Staiger and Apel, 1999).

### Plant growth

Arabidopsis seeds were surface-sterilized, stratified at 4°C for 2 days, germinated and grown on MS medium supplemented with 0.5% sucrose under 16 h light/8 h dark cycles at a constant temperature of 20°C. After about 10 days, seedlings of comparable size were transferred to fresh MS plates without sucrose.

Alternatively, seeds were sown on soil, stratified at 4°C for 2 days, and grown in an environmentally controlled growth room under

16 h light/8 h dark cycles at 20°C. After about 10 days, seedlings of comparable size were transferred to individual pots.

### RNA preparation

Total RNA for FDD, Northern blots, RT-PCR and quantitative RT-PCR was isolated as described previously (Staiger *et al.*, 2003b).

### Fluorescent differential display

First-strand cDNA was synthesized from 2.5  $\mu$ g of total RNA using the Texas Red-labelled 3'-anchored oligo(dT) primer (5'-Texas Red-gT15-A-3; Nisshinbo; <http://www.nisshinbo.co.jp>) and a SuperScript pre-amplification system (Gibco BRL; <http://invitrogen.com>).

PCR was performed using the anchored primer and arbitrary 10-mer primers (Operon Technologies; <http://www.operon.com>) using one cycle of 3 min at 94°C, 5 min at 40°C and 5 min at 72°C, 24 cycles of 15 sec at 94°C, 2 min at 40°C and 1 min at 72°C, and an 5 min extension at 72°C (Kuno *et al.*, 2000). Electrophoresis was performed using an automated fluorescent DNA sequencer (SQ 5500, Hitachi; <http://www.hitachi.com>).

To recover the bands, preparative electrophoresis was performed and the bands were visualized by a fluorescent image analyser (FMBIO II Multi-View, TaKaRa; <http://www.takara-bio.com>). cDNAs were eluted into H<sub>2</sub>O by freezing and thawing, re-amplified, and subcloned into the pGEM-T vector (Promega, <http://www.promega.com/>).

### RNA gel blot

Northern blotting and hybridization were carried out as described previously (Staiger *et al.*, 2003b). The gene-specific AtGRP7 and AtGRP8 probes are derived from the 5' UTR (Heintzen *et al.*, 1997). Primers for generation of the AtTLL1 and AtALP1 probes are listed in Table S1.

### Immunoblot analysis

Protein extraction and Western blots with chemiluminescence detection were performed as described previously (Heintzen *et al.*, 1997).

### Quantitative real-time PCR

Duplicate samples were analysed in a MJ Research opticon cycler (<http://www.biorad.com>). DNase I-treated RNA was reverse-transcribed, and 20 ng of retrotranscribed RNA was amplified using the Eppendorf Real MasterMix (<http://www.eppendorf.com>) kit for 2 min at 94°C, followed by 45 cycles of 20 sec at 94°C, 30 sec at 60°C and 40 sec at 68°C. Data were normalized to transcripts encoding eIF-4A-1 (At3g13920) or a PPR protein (At5g55840; Czechowski *et al.*, 2005). Expression levels in transgenic plants were normalized to WT in each experiment with respect to the reference genes. Primers are listed in Table S1. The absence of amplification products from genomic DNA was confirmed in a non-retrotranscribed control.

### Acknowledgements

We are indebted to Dr Brendan Davies (University of Leeds, UK) for the kind gift of *upf1* and *upf3* mutants and valuable discussions. We

thank Elisabeth Detring and Kristina Neudorf for expert technical assistance, and Christiane Theiss for purifying the fusion proteins for CD measurements. We are indebted to Christian Kambach (Paul Scherrer Institute, Villigen, Switzerland) for helpful discussions, and to Christian Heintzen (University of Manchester, UK) and Judith Gomez-Porras (University of Bielefeld, Bielefeld, Germany) for critical comments on the manuscript. J.C.S. is a fellow of the German National Academic Foundation. This work was supported by grants from the Deutsche Forschungsgemeinschaft (STA 653/2 and SFB 613) to D.S., from the Hitachi Advanced Research Laboratory (B2023) and the Program for Promotion of Basic Research Activity for Innovative Biosciences (1995–2000) to M.F., and from the Deutsche Forschungsgemeinschaft (Wo-695/3) to E.W.

### Supplementary Materials

The following supplementary material is available for this article online:

**Figure S1.** *AtGRP7* 3' UTR point mutations interfere with binding.

**Figure S2.** *AtGRP7* intron point mutations interfere with binding.

**Figure S3.** The secondary structures of *AtGRP7* and *AtGRP7*-RQ are almost identical.

**Figure S4.** FDD screen of *AtGRP7*-ox and WT RNA using the C anchor primer and arbitrary primers A1, A2, A3 and A4.

**Figure S5.** *AtGRP8* 3' UTR point mutations interfere with binding.

**Figure S6.** *AtGRP8* intron point mutations interfere with binding.

**Table S1.** Primers used in this study.

This material is available as part of the online article from <http://www.blackwell-synergy.com>.

### References

- Alabadi, D., Oyama, T., Yanovsky, M.J., Harmon, F.G., Mas, P. and Kay, S.A. (2001) Reciprocal regulation between TOC1 and LHY/CCA1 within the Arabidopsis circadian clock. *Science*, **293**, 880–883.
- Arciga-Reyes, L., Wootton, L., Kieffer, M. and Davies, B. (2006) UPF1 is required for nonsense-mediated mRNA decay (NMD) and RNAi in Arabidopsis. *Plant J.* **47**, 480–489.
- Brown, S.A. and Schibler, U. (1999) The ins and outs of circadian timekeeping. *Curr. Opin. Genet. Dev.* **9**, 588–594.
- Cao, S., Jiang, L., Song, S., Jing, R. and Xu, G. (2006) AtGRP7 is involved in the regulation of abscisic acid and stress responses in Arabidopsis. *Cell. Mol. Biol. Lett.* **11**, 526–535.
- Carpenter, C.D., Kreps, J.A. and Simon, A.E. (1994) Genes encoding glycine-rich Arabidopsis thaliana proteins with RNA-binding motifs are influenced by cold treatment and an endogenous circadian rhythm. *Plant Physiol.* **104**, 1015–1025.
- Chang, Y.F., Imam, J.S. and Wilkinson, M.F. (2007) The nonsense-mediated decay RNA surveillance pathway. *Annu. Rev. Biochem.* **76**, 51–74.
- Czechowski, T., Stitt, M., Altmann, T., Udvardi, M.K. and Scheible, W.R. (2005) Genome-wide identification and testing of superior reference genes for transcript normalization in Arabidopsis. *Plant Physiol.* **139**, 5–17.
- Ding, J., Hayashi, M.K., Zhang, Y., Manche, L., Krainer, A.R. and Xu, R.M. (1999) Crystal structure of the two-RRM domain of hnRNP A1 (UP1) complexed with single-stranded telomeric DNA. *Genes Dev.* **13**, 1102–1115.
- Dodd, A.N., Salathia, N., Hall, A., Kevei, E., Toth, R., Nagy, F., Hibberd, J.M., Millar, A.J. and Webb, A.A. (2005) Plant circadian clocks increase photosynthesis, growth, survival, and competitive advantage. *Science*, **309**, 630–633.
- Dodd, A.N., Jakobsen, M.K., Baker, A.J., Telzerow, A., Hou, S.W., Laplaze, L., Barrot, L., Scott Poethig, R., Haseloff, J. and Webb, A.A. (2006) Time of day modulates low-temperature Ca signals in Arabidopsis. *Plant J.* **48**, 962–973.
- Eastmond, P.J. (2004) Cloning and characterization of the acid lipase from castor beans. *J. Biol. Chem.* **279**, 45540–45545.
- Ederly, I. (1999) Role of posttranscriptional regulation in circadian clocks: lessons from Drosophila. *Chronobiol. Int.* **16**, 377–414.
- Edwards, K.D., Anderson, P.E., Hall, A., Salathia, N.S., Locke, J.C., Lynn, J.R., Straume, M., Smith, J.Q. and Millar, A.J. (2006) FLOWERING LOCUS C mediates natural variation in the high-temperature response of the Arabidopsis circadian clock. *Plant Cell*, **18**, 639–650.
- Falk, A., Feys, B.J., Frost, L.N., Jones, J.D.G., Daniels, M.J. and Parker, J.E. (1999) EDS1, an essential component of R gene-mediated disease resistance in Arabidopsis has homology to eukaryotic lipases. *Proc. Natl Acad. Sci. USA*, **96**, 3292–3297.
- Fu, Z.Q., Guo, M., Jeong, B., Tian, F., Elthon, T.E., Cerny, R.L., Staiger, D. and Alfano, J.R. (2007) A type III effector modifies RNA-binding proteins and quells plant immunity. *Nature*, **447**, 284–288.
- Gachon, F., Fonjallaz, P., Damiola, F., Gos, P., Kodama, T., Zakany, J., Duboule, D., Petit, B., Tafti, M. and Schibler, U. (2004) The loss of circadian PAR bZip transcription factors results in epilepsy. *Genes Dev.* **18**, 1397–1412.
- Gachon, F., Olela, F.F., Schaad, O., Descombes, P. and Schibler, U. (2006) The circadian PAR-domain basic leucine zipper transcription factors DBP, TEF, and HLF modulate basal and inducible xenobiotic detoxification. *Cell Metab.* **4**, 25–36.
- Green, R.M., Tingay, S., Wang, Z.-Y. and Tobin, E.M. (2002) Circadian rhythms confer a higher level of fitness to Arabidopsis plants. *Plant Physiol.* **129**, 576–584.
- Hall, A. and McWatters, H. (2006) *Endogenous Plant Rhythms*. Oxford, UK: Blackwell Publishing.
- Heintzen, C., Melzer, S., Fischer, R., Kappeler, S., Apel, K. and Staiger, D. (1994) A light- and temperature-entrained circadian clock controls expression of transcripts encoding nuclear proteins with homology to RNA-binding proteins in meristematic tissue. *Plant J.* **5**, 799–813.
- Heintzen, C., Nater, M., Apel, K. and Staiger, D. (1997) AtGRP7, a nuclear RNA-binding protein as a component of a circadian-regulated negative feedback loop in Arabidopsis thaliana. *Proc. Natl Acad. Sci. USA*, **94**, 8515–8520.
- Hori, K. and Watanabe, Y. (2005) UPF3 suppresses aberrant spliced mRNA in Arabidopsis. *Plant J.* **43**, 530–540.
- Iliev, D., Voytsekh, O., Schmidt, E.M., Fiedler, M., Nykytenko, A. and Mittag, M. (2006) A heteromeric RNA-binding protein is involved in maintaining acrophase and period of the circadian clock. *Plant Physiol.* **142**, 797–806.
- Jakab, G., Manrique, A., Zimmerli, L., Metraux, J.P. and Mauch-Mani, B. (2003) Molecular characterization of a novel lipase-like pathogen-inducible gene family of Arabidopsis. *Plant Physiol.* **132**, 2230–2239.
- Jessen, T.H., Oubridge, C., Teo, C.-H., Pritchard, C. and Nagai, K. (1991) Identification of molecular contacts between the U1A small nuclear ribonucleoprotein and U1 RNA. *EMBO J.* **10**, 3447–3456.
- Kertesz, S., Kerényi, Z., Merai, Z., Bartos, I., Palfy, T., Barta, E. and Silhavy, D. (2006) Both introns and long 3'-UTRs operate as cis-acting elements to trigger nonsense-mediated decay in plants. *Nucleic Acids Res.* **34**, 6147–6157.
- Kojima, S., Matsumoto, K., Hirose, M. et al. (2007) LARK activates posttranscriptional expression of an essential mammalian clock protein, PERIOD1. *Proc. Natl Acad. Sci. USA*, **104**, 1859–1864.

- Kuno, N., Muramatsu, T., Hamazato, F. and Furuya, M. (2000) Identification by large-scale screening of phytochrome-regulated genes in etiolated seedlings of *Arabidopsis* using a fluorescent differential display technique. *Plant Physiol.* **122**, 15–24.
- Law, M.J., Chambers, E.J., Katsamba, P.S., Haworth, I.S. and Laird-Offringa, I.A. (2005) Kinetic analysis of the role of the tyrosine 13, phenylalanine 56 and glutamine 54 network in the U1A/U1 hairpin II interaction. *Nucleic Acids Res.* **33**, 2917–2928.
- Lee, A.L., Volkman, B.F., Robertson, S.A., Rudner, D.Z., Barbash, D.A., Cline, T.W., Kanaar, R., Rio, D.C. and Wemmer, D.E. (1997) Chemical shift mapping of the RNA-binding interface of the multiple-RBD protein *sex-lethal*. *Biochemistry*, **36**, 14306–14317.
- Locke, J.C., Southern, M.M., Kozma-Bognar, L., Hibberd, V., Brown, P.E., Turner, M.S. and Millar, A.J. (2005) Extension of a genetic network model by iterative experimentation and mathematical analysis. *Mol. Syst. Biol.* Available at: <http://dx.doi.org/10.1038/msb4100018>.
- Maris, C., Dominguez, C. and Allain, F.H. (2005) The RNA recognition motif, a plastic RNA-binding platform to regulate post-transcriptional gene expression. *FEBS J.* **272**, 2118–2131.
- McClung, C.R. (2006) Plant circadian rhythms. *Plant Cell*, **18**, 792–803.
- McNeil, G.P., Zhang, X., Genova, G. and Jackson, F.R. (1998) A molecular rhythm mediating circadian clock output in *Drosophila*. *Neuron*, **20**, 297–303.
- McNeil, G.P., Smith, F. and Galio, R. (2004) The *Drosophila* RNA-binding protein Lark is required for the organization of the actin cytoskeleton and Hu-li Tai Shao localization during oogenesis. *Genesis*, **40**, 90–100.
- Mizuno, T. and Nakamichi, N. (2005) Pseudo response regulators (PRR) or true oscillator components (TOC). *Plant Cell Physiol.* **46**, 677–685.
- Morgenstern, B. (2004) DIALIGN: multiple DNA and protein sequence alignment at BiBiServ. *Nucleic Acids Res.* **32**, W33–W36.
- Nagai, K., Oubridge, C., Jessen, T.H., Li, J. and Evans, P.R. (1990) Crystal structure of the RNA-binding domain of the U1 small nuclear ribonucleoprotein A. *Nature*, **348**, 515–520.
- Rudolf, F., Wehrle, F. and Staiger, D. (2004) Slave to the rhythm. *Biochemist*, **26**, 11–13.
- Salome, P.A. and McClung, C.R. (2005) PSEUDO-RESPONSE REGULATOR 7 and 9 are partially redundant genes essential for the temperature responsiveness of the *Arabidopsis* circadian clock. *Plant Cell*, **17**, 791–803.
- Schaffer, R., Ramsay, N., Samach, A., Putterill, J., Carre, I.A. and Coupland, G. (1998) The late elongated hypocotyl mutation of *Arabidopsis* disrupts circadian rhythms and the photoperiodic control of flowering. *Cell*, **93**, 1219–1229.
- So, W.V. and Rosbash, M. (1997) Post-transcriptional regulation contributes to *Drosophila* clock gene mRNA cycling. *EMBO J.* **16**, 7146–7155.
- Staiger, D. and Apel, K. (1999) Circadian clock-regulated expression of an RNA-binding protein in *Arabidopsis*: characterisation of a minimal promoter element. *Mol. Gen. Genet.* **261**, 811–819.
- Staiger, D., Apel, K. and Trepp, G. (1999) The *Atger3* promoter confers circadian clock-regulated transcription with peak expression at the beginning of the night. *Plant Mol. Biol.* **40**, 873–882.
- Staiger, D., Zecca, L., Wiczeorek Kirk, D.A., Apel, K. and Eckstein, L. (2003a) The circadian clock regulated RNA-binding protein AtGRP7 autoregulates its expression by influencing alternative splicing of its own pre-mRNA. *Plant J.* **33**, 361–371.
- Staiger, D., Allenbach, L., Salathia, N., Fiechter, V., Davis, S.J., Millar, A.J., Chory, J. and Fankhauser, C. (2003b) The *Arabidopsis* *SRR1* gene mediates phyB signaling and is required for normal circadian clock function. *Genes Dev.* **17**, 256–268.
- Staiger, D., Streitner, C., Rudolf, F. and Huang, X. (2006) Multiple and slave oscillators. In *Endogenous Plant Rhythms* (Hall, A. and McWatters, H., eds). Oxford, UK: Blackwell Publishing, pp. 57–83.
- Steffen, P., Voss, B., Rehmsmeier, M., Reeder, J. and Giegerich, R. (2006) RNASHAPES: an integrated RNA analysis package based on abstract shapes. *Bioinformatics*, **22**, 500–503.
- Stitzinger, S.M., Conrad, T.R., Zachlin, A.M. and Salz, H.K. (1999) Functional analysis of SNF, the *Drosophila* U1A/U2B' homolog: identification of dispensable and indispensable motifs for both snRNP assembly and function *in vivo*. *RNA*, **5**, 1440–1450.
- Tang, Y. and Nilsson, L. (1999) Molecular dynamics simulations of the complex between human U1A protein and hairpin II of U1 small nuclear RNA and of free RNA in solution. *Biophys. J.* **77**, 1284–1305.
- Thompson, J.D., Higgins, D.G. and Gibson, T.J. (1994) CLUSTAL W: improving the sensitivity of progressive multiple sequence alignment through sequence weighting, position-specific gap penalties and weight matrix choice. *Nucleic Acids Res.* **22**, 4673–4680.
- Wang, Z.Y. and Tobin, E.M. (1998) Constitutive expression of the CIRCADIAN CLOCK ASSOCIATED1 (CCA1) gene disrupts circadian rhythms and suppresses its own expression. *Cell*, **93**, 1207–1217.
- Zhao, B., Schneid, C., Iliev, D., Schmidt, E.M., Wagner, V., Wollnik, F. and Mittag, M. (2004) The circadian RNA-binding protein CHLAMY 1 represents a novel type heteromer of RNA recognition motif and lysine homology domain-containing subunits. *Eukaryot. Cell*, **3**, 815–825.
- Zimmermann, P., Hirsch-Hoffmann, M., Hennig, L. and Gruissem, W. (2004) GENEVESTIGATOR. *Arabidopsis* microarray database and analysis toolbox. *Plant Physiol.* **136**, 2621–2632.
- Zuker, M. (2003) Mfold web server for nucleic acid folding and hybridization prediction. *Nucleic Acids Res.* **31**, 3406–3415.